

Portland State University

PDXScholar

Electrical and Computer Engineering Faculty
Publications and Presentations

Electrical and Computer Engineering

12-1-2009

Gain Guiding in Large-Core Bragg Fibers

Xianyu Ao

University of North Carolina at Charlotte

Tsing-Hua Her

University of North Carolina at Charlotte

Lee W. Casperson

Portland State University

Follow this and additional works at: https://pdxscholar.library.pdx.edu/ece_fac



Part of the [Electrical and Computer Engineering Commons](#)

Let us know how access to this document benefits you.

Citation Details

Xianyu Ao, Tsing-Hua Her, and Lee W. Casperson, "Gain guiding in large-core Bragg fibers," *Opt. Express* 17, 22666-22672 (2009).

This Article is brought to you for free and open access. It has been accepted for inclusion in Electrical and Computer Engineering Faculty Publications and Presentations by an authorized administrator of PDXScholar. Please contact us if we can make this document more accessible: pdxscholar@pdx.edu.

Gain guiding in large-core Bragg fibers

Xianyu Ao¹, Tsing-Hua Her^{1*}, and Lee W. Casperson²

¹*Department of Physics and Optical Science, and Center for Optoelectronics and Optical Communications, The University of North Carolina at Charlotte, 9201 University City Boulevard, Charlotte, NC 28223, USA*

²*Department of Electrical and Computer Engineering, and Center for Optoelectronics and Optical Communications, The University of North Carolina at Charlotte, 9201 University City Boulevard, Charlotte, NC 28223, USA*

*ther@uncc.edu

Abstract: We theoretically analyze gain guiding in large-core Bragg fibers, to be used for large-mode-area laser amplifiers with single-transverse-mode operation. The signal is gain-guided in a low-index core, whereas the pump is guided by the photonic bandgap of the Bragg cladding to achieve good confinement. The high-index layers in the Bragg cladding are half-wave thick at the signal wavelength in order to eliminate Bragg reflection, reducing the Bragg fiber effectively to a step-index fiber for gain guiding.

©2009 Optical Society of America

OCIS codes: (060.2320) Fiber optics amplifiers and oscillators; (060.4005) Microstructured fibers; (060.5295) Photonic crystal fibers; (160.5293) Photonic bandgap materials.

References and links

1. A. E. Siegman, "Propagating modes in gain-guided optical fibers," *J. Opt. Soc. Am. B* **20**(8), 1617 (2003).
2. A. E. Siegman, "Gain-guided, index-antiguidded fiber lasers," *J. Opt. Soc. Am. B* **24**(8), 1677 (2007).
3. A. E. Siegman, Y. Chen, V. Sudesh, M. C. Richardson, M. Bass, P. Foy, W. Hawkins, and J. Ballato, "Confined propagation and near single-mode laser oscillation in a gain-guided, index antiguided optical fiber," *Appl. Phys. Lett.* **89**(25), 251101 (2006).
4. Y. Chen, T. McComb, V. Sudesh, M. Richardson, and M. Bass, "Very large-core, single-mode, gain-guided, index-antiguidded fiber lasers," *Opt. Lett.* **32**(17), 2505–2507 (2007).
5. V. Sudesh, T. McComb, Y. Chen, M. Bass, M. Richardson, J. Ballato, and A. E. Siegman, "Diode-pumped 200 μm diameter core, gain-guided, index-antiguidded single mode fiber laser," *Appl. Phys. B* **90**(3-4), 369–372 (2008).
6. T.-H. Her, "Gain-guiding in transverse grating waveguides for large modal area laser amplifiers," *Opt. Express* **16**(10), 7197–7202 (2008).
7. P. Yeh, A. Yariv, and E. Marom, "Theory of Bragg fiber," *J. Opt. Soc. Am.* **68**(9), 1196 (1978).
8. B. Temelkuran, S. D. Hart, G. Benoit, J. D. Joannopoulos, and Y. Fink, "Wavelength-scalable hollow optical fibres with large photonic bandgaps for CO₂ laser transmission," *Nature* **420**(6916), 650–653 (2002).
9. G. Vienne, Y. Xu, C. Jakobsen, H.-J. Deyerl, J. Jensen, T. Sorensen, T. P. Hansen, Y. Huang, M. Terrel, R. K. Lee, N. A. Mortensen, J. Broeng, H. Simonsen, A. Bjarklev, and A. Yariv, "Ultra-large bandwidth hollow-core guiding in all-silica Bragg fibers with nano-supports," *Opt. Express* **12**(15), 3500–3508 (2004).
10. S. Février, R. Jamier, J.-M. Blondy, S. L. Semjonov, M. E. Likhachev, M. M. Bubnov, E. M. Dianov, V. F. Khopin, M. Y. Salganskii, and A. N. Guryanov, "Low-loss singlemode large mode area all-silica photonic bandgap fiber," *Opt. Express* **14**(2), 562–569 (2006).
11. S. Février, D. D. Gaponov, P. Roy, M. E. Likhachev, S. L. Semjonov, M. M. Bubnov, E. M. Dianov, M. Y. Yashkov, V. F. Khopin, M. Y. Salganskii, and A. N. Guryanov, "High-power photonic-bandgap fiber laser," *Opt. Lett.* **33**(9), 989–991 (2008).
12. T. Katagiri, Y. Matsuura, and M. Miyagi, "All-solid single-mode Bragg fibers for compact fiber devices," *J. Lightwave Technol.* **24**(11), 4314–4318 (2006).
13. S. G. Johnson, M. Ibanescu, M. Skorobogatiy, O. Weisberg, T. Engeness, M. Soljacic, S. Jacobs, J. Joannopoulos, and Y. Fink, "Low-loss asymptotically single-mode propagation in large-core OmniGuide fibers," *Opt. Express* **9**(13), 748–779 (2001).
14. E. A. J. Marcatili, and R. A. Schmelzter, "Hollow metallic and dielectric waveguides for long distance optical transmission and lasers," *Bell Syst. Tech. J.* **43**, 1783 (1964).
15. P. Yeh, A. Yariv, and C. S. Hong, "Electromagnetic propagation in periodic stratified media. I. general theory," *J. Opt. Soc. Am.* **67**(4), 423 (1977).
16. Y. Xu, R. K. Lee, and A. Yariv, "Asymptotic analysis of Bragg fibers," *Opt. Lett.* **25**(24), 1756–1758 (2000).
17. H. A. Macleod, *Thin-Film Optical Filters* (IOP, Philadelphia, 2001).
18. T.-H. Her, X. Ao, and L. W. Casperson, "Gain saturation in gain-guided slab waveguides with large-index antiguiding," *Opt. Lett.* **34**(16), 2411–2413 (2009).

1. Introduction

Recently laser oscillation in gain-guided and index-antiguided fibers [1,2] has been demonstrated to exhibit near-diffraction-limit beam characteristics with core diameter up to 400 μm [3,4]. In an index-antiguided (IAG) fiber the core has a lower refractive index relative to the surrounding cladding, and light propagating in the core eventually leaks into the cladding. For the signal radiation, single-transverse-mode operation can be achieved by balancing the leakage loss and the provided gain inside the core [2]. However, such lasers are not efficient under end pumping since most of the launched pump power leaks into the cladding due to index antiguiding [5]. To mitigate this problem, we have proposed a scheme based on gain guiding in photonic bandgap (PBG) waveguides in which the pump is confined inside the core via the PBG effect, while the signal is gain-guided and index-antiguided in the same core. This scheme was illustrated in a one-dimensional transverse grating waveguide [6]. Since the signal and the pump share the same core, one can expect a large overlap factor between the modes of the signal and the pump. Gain-guided photonic bandgap waveguides, therefore, could have ultra-large mode area, robust single-transverse-mode operation, and high pump efficiency. Photonic bandgap fibers, such as Bragg fibers, would serve as more practical waveguides for gain guiding. A Bragg fiber [7] is composed of concentric layers of alternating high- and low-index materials (Bragg cladding) surrounding a core, followed by a uniform outer cladding (see Fig. 1). Bragg fibers have been fabricated by drawing [8,9] or deposition [10–12]. Most studies have focused on modal characteristics inside the PBG of the Bragg cladding, where the lowest loss mode could be either TE_{01} [13] or HE_{11} [11,12], depending on the fiber configuration.

In this paper, we investigate gain guiding in Bragg fibers in which the signal is gain-guided and index-antiguided in a low-index core, while the pump is confined by the PBG effects of the Bragg cladding. Gain-guided Bragg fibers can be used for large-mode-area laser oscillators or amplifiers. Here the Bragg cladding serves two purposes. Firstly, it has a wide bandgap at the pump wavelength to confine the pump efficiently with a finite number of Bragg layers, which usually requires a large contrast in refractive indices between high- and low-index layers. Secondly, the Bragg cladding has a passband at the signal wavelength such that the Bragg fiber becomes equivalent to an IAG fiber, where the HE_{11} mode has the lowest loss for a modest index contrast [14]. For an IAG fiber to have large modal gain while remain single transverse mode, large modal loss is essential, which requires small index contrast between the core and the cladding [2]. These two requirements on the Bragg cladding seem to be incompatible. We resolve this issue by making the high-index layer in the Bragg cladding half-wave thick at the signal wavelength. We show that, under such condition, the Bragg fiber reduces to a step-index fiber for the signal, and the properties of the Bragg cladding can be considered independently for the signal and the pump.

2. Theoretical analysis

For a large-core fiber with relatively thin Bragg layers, the Bragg cladding can be considered approximately planar, and its optical properties can be understood using the theory of light propagation in one-dimensional periodically stratified media [15,16]. The Bloch wavenumber K in the Bragg cladding (with refractive indices n_1 and n_2) can be determined by [15]

$$\cos(K\Lambda) = \cos(k_1 d_1) \cos(k_2 d_2) - \gamma \sin(k_1 d_1) \sin(k_2 d_2), \quad (1)$$

with

$$\gamma = \begin{cases} \frac{1}{2} \left(\frac{k_1}{k_2} + \frac{k_2}{k_1} \right) & \text{TE} \\ \frac{1}{2} \left(\frac{n_2^2 k_1}{n_1^2 k_2} + \frac{n_1^2 k_2}{n_2^2 k_1} \right) & \text{TM} \end{cases}, \quad (2)$$

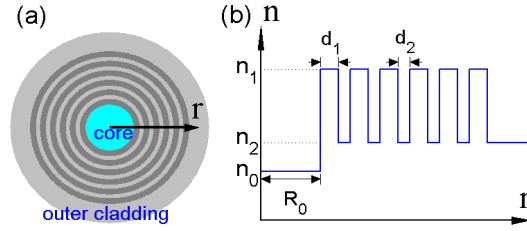


Fig. 1. Schematic of a Bragg fiber (a) and the radial index profile (b) (not to scale).

where $\Lambda = d_1 + d_2$ is the period of the Bragg layers, $k_j = \sqrt{(2\pi/\lambda)^2 n_j^2 - \beta^2}$ ($j = 1, 2$) is the transverse component of the wavevector in each layer, and β is the complex propagation constant of modes in the fiber.

For the signal to be gain-guided in a single transverse mode, its wavelength needs to be located inside the passing zones of the Bragg cladding for both TE and TM polarizations. One possible way to accomplish this is to impose $k_1 d_1 = \pi$ in Eq. (1) (*i.e.*, half-wave condition at the signal wavelength) such that $\cos(K\Lambda) = -\cos(k_2 d_2)$, which ensures the same real wavenumber in the Bragg cladding for both polarizations. Given glancing incidence of low-order modes in a large-core (with refractive index n_0) fiber where $\beta \approx \omega n_0/c$ (*i.e.*, the core light line), the thickness d_1 can be determined from the half-wave condition at the signal wavelength λ_s to be

$$d_1 = \lambda_s / 2\sqrt{n_1^2 - n_0^2}. \quad (3)$$

It is well known in thin-film optics that when a dielectric layer is half-wave thick, it becomes an absentee layer such that its presence does not affect optical properties of the whole structure [17]. Since in the current Bragg fibers the n_1 layers are half-wave thick, we expect that they become absentee layers to the low-order modes such that the Bragg cladding reduces effectively to a uniform cladding with refractive index n_2 . This can be seen by examining the mode fields and the dispersion equation of a Bragg fiber under the conditions of $R_0 \gg \Lambda$ and $k_1 d_1 = \pi$. The radial dependence of the E_z field in a Bragg fiber can be written as (in the cladding the asymptotic expressions are used for the Hankel functions) [16],

$$E_z(r) = a_c J_m(k_0 r), \quad r \leq R_0, \quad (4a)$$

$$E_z(r) = \frac{a'_l \exp[ik_1(r - R_l)] + b'_l \exp[-ik_1(r - R_l)]}{\sqrt{k_1 r}}, \quad R_l \leq r \leq R_l + d_1, \quad (4b)$$

$$E_z(r) = \frac{a_l \exp[ik_2(r - R_l - d_1)] + b_l \exp[-ik_2(r - R_l - d_1)]}{\sqrt{k_2 r}}, \quad R_l + d_1 \leq r \leq R_l + \Lambda, \quad (4c)$$

where $R_l = R_0 + (l-1)\Lambda$ and $k_0 = \sqrt{(2\pi/\lambda)^2 n_0^2 - \beta^2}$ is the wavenumber in the core, and a_l, b_l (a'_l, b'_l) are the field coefficients in the n_2 (n_1) layer of the l -th period in the cladding. Similar expressions can be written for the H_z field with another set of expansion coefficients, and all other field components can be obtained from E_z and H_z . In the asymptotic limit, the coefficients a_l and b_l in the adjacent n_2 layers are related by a transfer matrix as in planar stratified media [15,16],

$$\begin{pmatrix} a_l \\ b_l \end{pmatrix} = \begin{bmatrix} A_{\text{TM}} & B_{\text{TM}} \\ B_{\text{TM}}^* & A_{\text{TM}}^* \end{bmatrix} \begin{pmatrix} a_{l+1} \\ b_{l+1} \end{pmatrix}, \quad (5)$$

with

$$A_{\text{TM}} = \exp(-ik_2 d_2) \left[\cos(k_1 d_1) - \frac{i}{2} \left(\frac{n_1^2 k_2}{n_2^2 k_1} + \frac{n_2^2 k_1}{k_2 n_1^2} \right) \sin(k_1 d_1) \right], \quad (6a)$$

$$B_{\text{TM}} = \exp(-ik_2 d_2) \left[\frac{i}{2} \left(\frac{n_2^2 k_1}{k_2 n_1^2} - \frac{n_1^2 k_2}{n_2^2 k_1} \right) \sin(k_1 d_1) \right]. \quad (6b)$$

Under the half-wave condition $k_1 d_1 = \pi$, B_{TM} is zero and the transfer matrix becomes diagonal. This indicates that the outgoing wave and incoming wave in the n_2 layers are decoupled. Since there is no incoming wave at infinity, we have $b_n = 0$ for all the n_2 layers. Similarly, there is no incoming wave for the H_z field in the n_2 layers. Consequently, the field expressions in the n_2 layers of the Bragg fiber reduce to those of a step-index fiber. In addition, by matching the boundary conditions and keeping only the $(k_j r)^{(-1/2)}$ terms for E_θ and H_θ [17], we obtain the following dispersion equation provided that $R_0 \gg \Lambda$ and $k_1 d_1 = \pi$,

$$\left(\frac{\beta m \lambda_s}{2\pi k_0 R_0 n_0} \right)^2 \left(1 - \frac{k_0^2}{k_2^2} \right)^2 = \left[\frac{J'_m(k_0 R_0)}{J_m(k_0 R_0)} - i \frac{\varepsilon_2 k_0}{\varepsilon_0 k_2} \right] \left[\frac{J'_m(k_0 R_0)}{J_m(k_0 R_0)} - i \frac{k_0}{k_2} \right]. \quad (7)$$

This dispersion equation is equivalent to the one for a step-index fiber in Ref [14], as in the asymptotic limit we have $H_m^{(1)}(k_2 R_0) / H_m^{(1)}(k_0 R_0) \rightarrow i$. Since both the field expressions and propagation constants are identical, the Bragg fiber indeed behaves like a step-index IAG fiber with a core index n_0 and a cladding index n_2 . The leakage loss of the signal in the Bragg fiber then follows that of the corresponding IAG fiber, which is determined by the dimensionless index parameter $\Delta N = (2\pi / \lambda_s)^2 \cdot R_0^2 \cdot (n_2^2 - n_0^2)$ [2]. Such leakage loss has shown to be critical in determining the saturated power in gain-guided IAG waveguides [18].

We now turn to the bandgap properties at the pump wavelength λ_p . To confine the pump efficiently, the Bragg cladding needs to have a complete bandgap at the pump wavelength, and it is beneficial to have a numerical aperture (NA) as large as possible to facilitate the coupling of the pump light into the Bragg fiber. Since the low-order modes of the pump also approach glancing incidence, the bandgaps of the one-dimensional Bragg cladding satisfy the following requirement [15] under the constraint of Eq. (3) [cf. Equation (1)],

$$|\cos(\varphi_1) \cos(\varphi_2) - \gamma \sin(\varphi_1) \sin(\varphi_2)| \geq 1, \quad (8)$$

where $\varphi_1 = \pi \lambda_s / \lambda_p$, $\varphi_2 = 2\pi d_2 (n_2^2 - n_0^2)^{1/2} / \lambda_p$. Equation (8) can be used to select the parameters of n_1 and d_2 to ensure that there is a complete bandgap at the pump wavelength. Since the bandgaps of the TE polarization usually cover those of the TM polarization, we may examine Eq. (8) for the TM polarization only.

3. Example and discussion

We apply the above principle to a Bragg fiber with 6 pairs of Bragg layers followed by an infinite outer cladding with the same refractive index as the low-index layer [see Fig. 1(b)]. The fiber has a core radius $R_0 = 50 \mu\text{m}$, refractive indices $n_0 = 1.56$, and $n_2 = 1.57$. The pump wavelength is $\lambda_p = 0.803 \mu\text{m}$ (as for a typical wavelength of diode lasers), and the signal wavelength is $\lambda_s = 1.055 \mu\text{m}$ (as for a Nd-doped glass fiber).

Figure 2(a) shows the combination of n_1 and d_2 for which there is a complete bandgap for the pump at glancing incidence [*i.e.*, for those n_1 and d_2 Eq. (8) is satisfied]. The band diagram of an infinite Bragg cladding for $n_1 = 2.2$ [the corresponding thickness d_1 determined from Eq. (3) is $0.34 \mu\text{m}$] and $d_2 = 0.575 \mu\text{m}$ is shown in Fig. 2(b). At the signal wavelength, the light line of the core is located inside the passing zones for both TE and TM polarizations, indicating the low-order modes are lossy in a passive fiber. At the pump wavelength, there is a

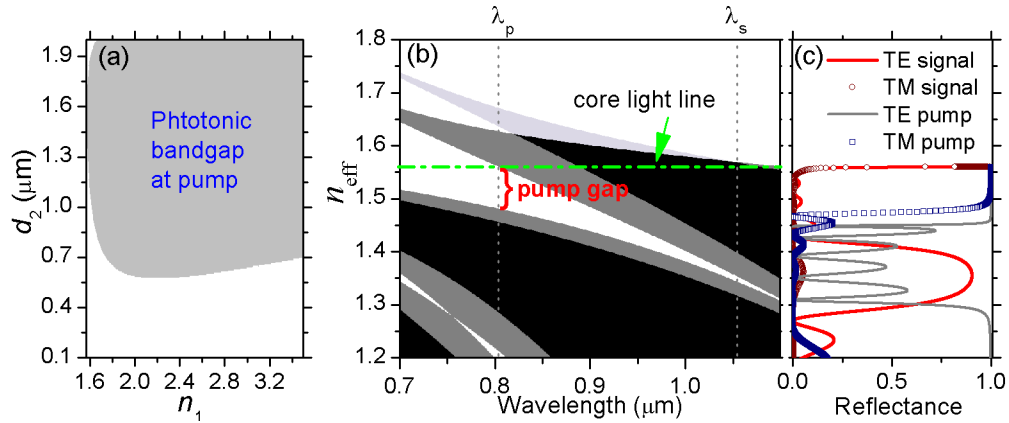


Fig. 2. (a) Combinations of n_1 and d_2 for which a complete bandgap exists for the pump at glancing incidence. Other parameters are fixed (see text). (b) Band diagram for $n_1 = 2.2$, $n_2 = 1.57$, $d_1 = 0.34 \mu\text{m}$, and $d_2 = 0.575 \mu\text{m}$. The shaded areas indicate allowed bands for TE polarization (light gray), TM polarization (dark gray), and overlaps (black). White areas indicate complete bandgaps. (c) Reflectance of a planar structure with the same index profile as in Fig. 1(b).

complete bandgap covering the range of $1.50 < n_{\text{eff}} < 1.56$, implying a quite large acceptance angle for the pump [$\text{NA} \approx 1.56 \times \sin(\cos^{-1}(1.50/1.56)) = 0.42$]. Notice that the small gap located near $n_{\text{eff}} = 1.35$ at the signal wavelength will not diminish the robustness of single-transverse-mode operation during the gain guiding, since these higher-order modes possess much higher loss in a Bragg fiber with a finite Bragg cladding. This is confirmed by examining the reflectance of a planar structure with the same index profile as in Fig. 1(b). As shown in Fig. 2(c), the signal has a much lower reflectance ($\sim 90\%$) near $n_{\text{eff}} = 1.35$ than at glancing incidence ($> 99\%$). Also indicated is the strong PBG effects at the pump wavelength (reflectance $> 99\%$ for both TE and TM polarizations) with only 6 pairs of Bragg layers.

Table 1 shows the complex effective indices of low-order modes of a Bragg fiber with 6 pairs of Bragg layers, calculated by a rigorous transfer matrix method based on the Bessel function expansion [7]. Also shown are results for the corresponding IAG fiber, calculated by the analytical formula in Ref [14]. The loss of the pump is overall three orders of magnitude smaller than that of the signal in the Bragg fiber, indicating good pump confinement. The complex effective indices are nearly identical for the Bragg fiber and the corresponding IAG fiber at the signal wavelength, indicating the high-index layers indeed have no effect in the Bragg fiber. This is further confirmed by the overlapped radial profiles of S_z of the HE_{11} mode for both fibers, as shown in Fig. 3(a). The inset of Fig. 3(a) also shows the radial phase profile of the H_z field in the Bragg cladding, indicating a π -phase shift over each n_1 layer. This is consistent with the imposed half-wave condition. Notice that the loss coefficient of the LP_{11} mode is about 2.5 times higher than that of the LP_{01} mode in the Bragg fiber, which is very promising for strong transverse mode discrimination during gain guiding [2]. Furthermore, the modal gain coefficient of the Bragg fiber is identical to that of the IAG fiber when the material gain is present in the core, as shown in Fig. 3(b). For the current example where $-AN \sim 2000$, the mode profile is expected to show little change before and after the onset of gain guiding [2].

Table 1. Modal Properties of an IAG Fiber and a Bragg Fiber with 6 pairs of Bragg Layers.

Mode	IAG signal [†]		Bragg signal		Bragg pump
	Effective index	Loss (cm ⁻¹)	Effective index	Loss(cm ⁻¹)	Loss(cm ⁻¹)
HE ₁₁	1.5599790935	9.51×10^{-2}	1.5599791208	9.50×10^{-2}	5.60×10^{-5}
TE ₀₁	1.5599469235	2.40×10^{-1}	1.5599469927	2.40×10^{-1}	1.93×10^{-9}
TM ₀₁	1.5599469235	2.43×10^{-1}	1.5599469921	2.42×10^{-1}	2.83×10^{-4}
HE ₂₁	1.5599469235	2.41×10^{-1}	1.5599469918	2.41×10^{-1}	1.42×10^{-4}

[†] Calculated by the analytical formula in Ref [14].

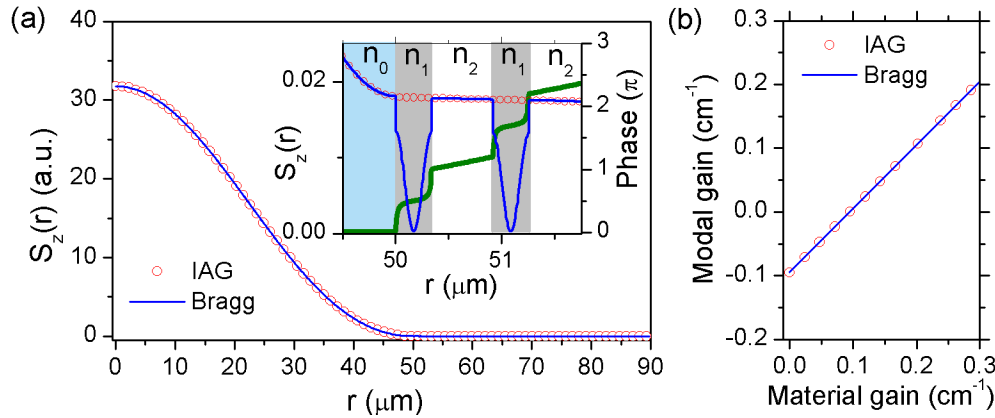


Fig. 3. (a) Radial profile of S_z of the HE₁₁ mode in an IAG fiber (open circles) and a Bragg fiber with 6 pairs of Bragg layers (blue solid line) at the signal wavelength. Inset shows the expanded view of S_z (left axis; open circles and blue line) and the radial phase profile of the H_z field in the Bragg cladding (right axis; green line). (b) Modal gain coefficient of the HE₁₁ mode as a function of the material gain for the IAG fiber (open circles) and a Bragg fiber (solid line).

It is also found that, when d_1 deviates from the designed value by $-1\% \sim +3\%$, the loss coefficients of TE₀₁, TM₀₁, and HE₂₁ modes for the signal remain close and are about 2 times larger than that of the HE₁₁ mode. This suggests fairly robust gain guiding with single transverse mode in this Bragg fiber even if the thickness of the high-index layers deviates from the half-wave condition slightly. A more judicious selection of n_1 and d_2 could improve the tolerance further. For the present example, a threshold gain of 0.1 cm^{-1} would require a doping density of $\sim 6 \times 10^{20} \text{ ions/cm}^3$ which may be obtained with 6 wt % Kigre Q98 glass. Bragg cladding of such design could be potentially realized using the techniques described in Refs. [8]. and [12].

4. Conclusion

We have analyzed theoretically gain guiding in a large-core Bragg fiber, in which the signal is gain-guided and index-antiguided in the fiber core, while the pump is confined in the same core by the photonic bandgaps of the Bragg cladding. We imposed a half-wave condition on the high-index layers in the Bragg cladding such that they have no effect on fiber modes at the signal wavelength. Under this condition, the low-order modes of the signal in the Bragg fiber and the corresponding IAG fiber have nearly identical propagation constants and mode fields, as well as modal gains when gain guiding. The loss at the signal wavelength can then be solely determined by the index contrast between the core and the low-index layers of the Bragg cladding, while the high-index layers are used to optimize the photonic bandgap at the pump wavelength. This half-wave condition is expected to substantially simplify the design of gain-guided Bragg fibers, which hold promise for high-power laser amplifiers and oscillators with robust single transverse mode and large mode area.

Acknowledgments

This work is supported by DARPA under Young Faculty Award No. HR0011-08-1-0065 and National Science Foundation under Grant No. 0925992.